Journal of
Mechanics of
Materials and Structures

OPTIMIZATION OF PENETRATION INTO GEOLOGICAL AND CONCRETE SHIELDS BY IMPACTOR WITH JET THRUSTER

Gabi Ben-Dor, Anatoly Dubinsky and Tov Elperin

Volume 3, Nº 4 April 2008

mathematical sciences publishers

JOURNAL OF MECHANICS OF MATERIALS AND STRUCTURES
Vol. 3, No. 4, 2008

OPTIMIZATION OF PENETRATION INTO GEOLOGICAL AND CONCRETE SHIELDS BY IMPACTOR WITH JET THRUSTER

GABI BEN-DOR, ANATOLY DUBINSKY AND TOV ELPERIN

High-speed penetration into soil, rock, concrete, and ice by impactors equipped with a jet thruster is optimized using analytical and numerical methods. It is shown that using a jet thruster with optimum burning programs bears considerable promise for increasing the depth of penetration. In this study, we used modified Young's penetration equations with a smooth approximation of the dependence between the depth of penetration and impact velocity for the description of impactor-shield interaction.

1. Introduction

Optimization of jet propulsion in media with drag was considered mainly with applications to planes and missiles. Surveys of the obtained results and references can be found in the studies by Leitmann [1962], Kosmodemiansky [1966], and Tertychny-Dauri [2004]. Using jet thrusters for increasing the depth of penetration into solid media was analyzed in only a few publications. Sagomonyan [1988] formulated two problems. In the first problem, a jet thruster was assumed to operate during a fixed time interval, and, in order to maximize the depth of penetration (DOP) of penetrator into soil, it was necessary to determine the moment at which the jet thruster must be switched on. In the second problem, a jet thruster could operate along a fixed length of the trajectory, and, in order to provide the maximum DOP, it was necessary to determine the depth at which the jet thruster must be switched on. The second problem was solved for a penetrator with a conical nose, assuming that the mass of the penetrator remains constant. Gould [1997] suggested engineering designs whereby a rocket motor is attached to the penetrator and operates during penetration. Ben-Dor et al. [2007] considered maximization of the DOP as an optimization problem for a penetrator with a variable mass. They noticed a similarity between this problem and maximization of the distance of a horizontal flight in the atmosphere. Various formulations of the latter problem were considered in the past [Hibbs 1952; Cicala and Miele 1956; Miele 1957; Miele 1962; Krotov 1995]. However, it transpired that this similarity had limited applications because of different drag laws in the atmosphere and soil. Only general properties of the solutions obtained for an arbitrary dependence of drag force upon the instantaneous mass and velocity, $D = D(m, v)$, can be used for solving penetration optimization problems. Consequently, optimization of the penetrator with a jet thruster must be analyzed separately. In the study by Ben-Dor et al. [2007], the authors employed the simplest penetration model in which the drag force is a linear function of a squared velocity. Combining analytical and numerical methods, they determined the optimum burning programs and compared the obtained results with more simple burning programs for controlling the motion of a penetrator.

Keywords: rock, concrete, soil, penetration, optimization, jet thruster.

In the present study, we further develop the approach suggested in [Ben-Dor et al. 2007] for a penetration model with a drag force depending upon the instantaneous velocity and the instantaneous mass of the impactor, whereby, as often happens in practice, the dependence of the drag force in different intervals of its arguments may be determined by different formulas. As a base model, we employed the well known set of models suggested by Young [1997] which is widely used for calculating the DOP in soil, rock, concrete, ice, and frozen soil. The shortcoming of these models is a nonsmooth variation of the DOP with impact velocity which is especially inconvenient in solving optimization problems. Consequently, we suggested a new approximation which is practically as simple and accurate as the original one but has continuous first and second derivatives. The latter renders this approximation more convenient, not only for the goals of the present study, but also for general applications. For a drag force determined by this modified Young's model (MYM), we analytically found the optimal burning programs for the case without an upper bound on the mass flux of the thruster. We suggested a numerical procedure based on dynamic programming for the optimization of the burning program for the general case of $D = D(m, v)$ and a tailored version of this procedure for (MYM). Calculations presented here demonstrate that the appropriate choice of parameters for the jet thruster allows achieving a considerable increase of the DOP.

2. Formulation of the problem

Consider a high speed normal penetration of a rigid sharp striker (a body of revolution) with a jet thruster into a semiinfinite shield along the axis h. The coordinate h, the instantaneous depth of penetration, is defined as the distance between the nose of the impactor and the front surface of the shield.

Since the effect of gravity during high speed penetration in a dense medium can be neglected, motion of the impactor is governed by the following equation of motion of a projectile with a variable mass:

$$m\frac{dv}{dt} + c\frac{dm}{dt} = -D(m, v), \qquad D(m, v) > 0, \tag{1}$$

where v is the velocity of the impactor, c is the relative exit velocity of gases at the nozzle of a jet thruster, m is the instantaneous mass of the impactor that varies in the range between the initial value m_{imp} to the final value m_{res}, that is,

$$m_{\text{res}} \le m \le m_{\text{imp}}, \tag{2}$$

and D is the drag force depending not only on m and v, but also on parameters determining mechanical properties of the shield and the shape of the projectile.

It is assumed that the thruster is capable of delivering all mass fluxes in the range between zero and the maximum value $\mu_{\max}$:

$$-\mu_{\max} \le \frac{dm}{dt} \le 0. \tag{3}$$

The constraint imposed on the acceleration is as follows:

$$|dv/dt| \le \chi_{\max} g, \tag{4}$$

where g is the acceleration of gravity, and $\chi_{\max}$ is the given upper bound for the overload of the impactor.

Since $d/dt = (d/dh)\cdot(dh/dt) = vd/dh = v(dm/dh)\cdot(d/dm)$, Equation (1) can be rewritten as follows:

$$v\frac{dm}{dh}(mv'+c) = -D(m,v), \qquad v' = \frac{dv}{dm}. \tag{5}$$

The DOP, H, for a given impact velocity, v_{imp}, is defined as the depth at which the velocity of the impactor vanishes. Equation (5) implies the following expression for H:

$$H = \int_{m_{\text{res}}}^{m_{\text{imp}}} \frac{(mv'+c)v}{D(m,v)}dm. \tag{6}$$

We consider v to be a function of m. This is convenient because penetration is associated with a decrease of m, and v is a single-valued function of m except for the case in which $m = \text{const}$ (inertial, or passive motion of the penetrator). The following conditions are valid for the initial and terminal points of the impactor's path:

$$v(m_{\text{imp}}) = v_{\text{imp}}, \qquad v(m_{\text{res}}) = 0. \tag{7}$$

Using Equation (5) we obtain that

$$\frac{dm}{dt} = v\frac{dm}{dh} = -\frac{D(m,v)}{mv'+c}, \tag{8}$$

and Equation (3) can be rewritten as

$$0 \le \frac{D(m,v)}{mv'+c} \le \mu_{\max}. \tag{9}$$

Using the relationship $dt = -(c+mv')dm/D(m,v)$ obtained from Equation (8) we can rewrite Equation (3) in the form:

$$\left|\frac{D(m,v)v'}{mv'+c}\right| \le \chi_{\max}g. \tag{10}$$

We also assume that

$$v \ge 0, \qquad v \le v_{\max}, \tag{11}$$

where $v_{\max}$ is the maximum velocity of the impactor.

The problem is to determine the function $v(m)$ that provides the maximum DOP, H, in Equation (6), taking into account the constraints given by Equations (7), (9), (10) and (11). Function $D(m,v)$ and the parameters $\mu_{\max}$, $\chi_{\max}$, $v_{\max}$, m_{imp}, m_{res}, and v_{imp} are assumed to be given.

Inequalities in Equation (9) imply two situations: the possibility of the *vertical subarcs*, $m = \text{const}$ when $v' = \infty$, and the restrictions $mv'+c \ge D(m,,v)/\mu_{\max}$ and $mv'+c \ge 0$ when $v' < \infty$. Clearly, the latter inequality can be omitted and we can write this constraint as follows:

$$mv'+c \ge D(m,v)/\mu_{\max}, \qquad \text{if } v' < \infty. \tag{12}$$

For $m = \text{const}$ ($v' = \infty$), the constraint in Equation (10) can be simplified:

$$D(m,v)/m \le \chi_{\max}g, \qquad \text{if } m = \text{const}. \tag{13}$$

3. Generalized Young's penetration model

Numerous simplified models were proposed for high speed penetration into different media. An overview of these models may be found, for instance, in the recent monograph [Ben-Dor et al. 2006] and the review [Ben-Dor et al. 2005]. In this study are employed the well known Young's penetration equations [Young 1997] which determine the DOP into soil, rock, and concrete (SRC) shields as well as into ice and frozen soil (IFS) in the following unified form:

$$\frac{P(v_{\text{imp}})}{k} = \begin{cases} \tilde{P}_a(v_{\text{imp}}) & \text{if } v_{\text{imp}} < \tilde{v}_* \\ \tilde{P}_b(v_{\text{imp}}) & \text{if } v_{\text{imp}} \geq \tilde{v}_*, \end{cases} \tag{14}$$

where

$$\tilde{P}_a(v_{\text{imp}}) = \tilde{\alpha}_1 \ln(1 + \tilde{\alpha}_2 v_{\text{imp}}^2), \qquad \tilde{P}_b(v_{\text{imp}}) = k_1(v_{\text{imp}} - v_0), \tag{15}$$

$$k = k_0\theta(m), \qquad k_0 = \tilde{S}\tilde{N}/\tilde{A}^{\kappa_1}, \tag{16}$$

$$\theta(m) = \begin{cases} \sigma m^{\kappa_1+\kappa_2} & \text{if SRC} \\ m^{\kappa_1} \ln(50 + 0.29m^2) & \text{if IFS,} \end{cases} \tag{17}$$

P is the DOP, $\tilde{S}$ is a coefficient depending on the mechanical properties of the shield, $\tilde{N}$ depends on the shape of the impactor, $\tilde{A}$ is the cross sectional area of the impactor, $v_0 = 30.5$, $\tilde{\alpha}_2 = 0.000215$, $\tilde{v}_* = 2v_0 = 61$, other coefficients are presented in Table 1. It is assumed that the mass of the projectile is constant. The parameters of the model are chosen such that the variables are measured in SI units [Young 1997]. Unfortunately, this widely used model is inconvenient in theoretical analysis because it employs the dimensional coefficients and because it is described by a discontinuous function.

Indeed, Young's dependence in the range between $P/k = \hat{P}$ and v_{imp} for SRC is described by a function that is discontinuous at $v_{\text{imp}} = \tilde{v}_*$, $\tilde{P}_a(\tilde{v}_*) = 0.000470$, $P_b(\tilde{v}_*) = 0.000549$. Inaccuracy in calculation is a plausible reason for this discontinuity, and can be corrected by choosing $\tilde{\alpha}_1$ such that $\tilde{P}_a(\tilde{v}_*) = \tilde{P}_b(\tilde{v}_*)$. Then we obtain that

$$\tilde{\alpha}_1/k_1 = v_0/\ln(1 + \tilde{\alpha}_2 v_*^2) = 51.89. \tag{18}$$

The corrected values $\tilde{\alpha}_1$ that enforce the continuity of $\hat{P}(v_{\text{imp}})$ are presented in Table 1. However, in our study we need a more smooth approximation of the function $\hat{P}(v_{\text{imp}})$, namely, it must have the

Shield's material	m	κ_1	κ_2	σ	$\tilde{\alpha}_1$	k_1	$\tilde{\alpha}_1$, corrected
Soil	$2 \leq m < 27$	0.7	0.4	0.27	0.0008	0.000018	0.0009340
	$m \geq 27$	0.7	0	1	0.0008	0.000018	0.0009340
Rock, Concrete	$5 \leq m < 182$	0.7	0.15	0.46	0.0008	0.000018	0.0009340
	$m \geq 182$	0.7	0	1	0.0008	0.000018	0.0009340
Ice, Frozen Soil		0.6			0.00024	0.0000046	0.0002387

Table 1. Parameters of the models.

continuous second derivative for all $v_{\text{imp}} > 0$. Toward this end, we modify the model for the relatively small v_{imp} keeping the Young's approximation for large v_{imp}. We look for this approximation of the function $P(v_{\text{imp}})$ in the following form:

$$\frac{P(v_{\text{imp}})}{k} = \begin{cases} P_a(v_{\text{imp}}) & \text{if } v_{\text{imp}} < v_* \\ \tilde{P}_b(v_{\text{imp}}) & \text{if } v_{\text{imp}} \geq v_*, \end{cases} \tag{19}$$

where

$$P_a(v_{\text{imp}}) = \left(\alpha_2 v_{\text{imp}}^2 + \alpha_1 v_{\text{imp}} + \alpha_0\right) v_{\text{imp}}^2, \quad v_{\text{imp}} \leq v_* \tag{20}$$

$$v_* = s v_0, \quad s \geq 2. \tag{21}$$

The constraint in Equation (21) follows from the fact that the function $\tilde{P}_b(v_{\text{imp}})$ is defined only for $v_{\text{imp}} \geq \tilde{v}_* = 2v_0$.

The problem is to find such α_0, α_1, α_2, and v_* (or s) that

$$P_a(v_*) = \tilde{P}_b(v_*), \qquad P_a'(v_*) = \tilde{P}_b'(v_*), \qquad P_a''(v_*) = \tilde{P}_b''(v_*), \qquad v_* = s v_0, \tag{22}$$

where

$$\begin{aligned} P_a'(v_{\text{imp}}) &= 4\alpha_2 v_{\text{imp}}^3 + 3\alpha_1 v_{\text{imp}}^2 + 2\alpha_0 v_{\text{imp}}, & \tilde{P}_b'(v_{\text{imp}}) &= k_1, \\ P_a''(v_{\text{imp}}) &= 12\alpha_2 v_{\text{imp}}^2 + 6\alpha_1 v_{\text{imp}} + 2\alpha_0, & \tilde{P}_b''(v_{\text{imp}}) &= 0. \end{aligned} \tag{23}$$

In addition, by physical reasoning, P_a must be an increasing function.

Equation (22) yields a system of linear equations with respect to α_0, α_1, and α_2 which has the following solution:

$$\alpha_0 = \frac{3k_1(s-2)}{s^2 v_0}, \qquad \alpha_1 = \frac{k_1(8-3s)}{s^3 v_0^2}, \qquad \alpha_2 = \frac{k_1(s-3)}{s^4 v_0^3}. \tag{24}$$

Let us prove that for any $s \geq 2$, the function $P_a(v_{\text{imp}})$ increases when $0 < v_{\text{imp}} \leq s v_0$. This occurs if $P_a'(v_{\text{imp}}) > 0$ in the same range of v_{imp}, or if $\omega(V) > 0$ for $0 < V \leq 1$, where

$$\omega(V) = \frac{1}{k_1 v_0 V} P_a'(s v_0 V) = 4(s-3)V^2 + 3(8-3s)V + 6(s-2), \qquad V = \frac{v_{\text{imp}}}{s v_0}. \tag{25}$$

Let $2 \leq s < 3$. Since $\omega(0) \geq 0$ and $\omega(1) = s > 0$, the convex function $\omega(V) > 0$ for $0 < V \leq 1$.

The discriminant of the quadratic equation $\omega(V) = 0$ is $\Delta(s) = 3s(16-5s)$. Since $\Delta < 0$ and $s - 3 > 0$ when $s > 16/5$, then $\omega(V) > 0$ for $s > 16/5 = 3.2$.

Let $3 \leq s < 3.2$. Then there are two different roots of the equation $\omega(V) = 0$, V_1 and V_2. The Viet formula implies that both the roots are positive. The smaller root, V_1, is

$$V_1(s) = [3(3s-8) - \sqrt{\Delta(s)}]/[8(s-3)].$$

It is easy to prove that $V_1 > 1$ if $3 \leq s < 3.2$. Since $\omega(0) > 0$ and all the roots are larger than 1, $\omega(V) > 0$ for $0 < V \leq 1$.

In order to complete the analysis, let us consider $\omega(V)$ for two remaining values s. If $s = 3$ then $\omega(V) = 3(2 - V) > 0$, and if $s = 3.2$ then $\omega(V) = 0.8(V-3)^2 > 0$, for $0 < V \leq 1$.

Thus we proved that $P_a(v_{\text{imp}})$ is an increasing function for $0 < v_{\text{imp}} \leq s v_0$ when $s \geq 2$.

Smooth approximation of the function $P = P(v_{\text{imp}})$ in Equation (19) allows one to determine the dependence of the drag force, D, on the instantaneous velocity, v, that yields the following correlation for motion of the impactor with a constant mass m:

$$D = \frac{m}{k} \times \begin{cases} D_a & \text{if } v < v_*, \\ D_b & \text{if } v \geq v_*, \end{cases} \tag{26}$$

where

$$\begin{aligned} D_a(v) &= v/P_a'(v) = (4\alpha_2 v^2 + 3\alpha_1 v + 2\alpha_0)^{-1}, \\ D_b(v) &= v/\tilde{P}_b'(v) = v/k_1. \end{aligned} \tag{27}$$

The validity of this statement can be verified directly by determining the DOP from the equation of motion of the impactor, $mvdv/dh = -kD$. Equation (22) implies that the function D has a continuous derivative with respect to v. Note that a similar approach was used in [Eisler et al. 1998] for the case in which the dependence of the DOP on v_{imp} is determined by one analytical expression.

By physical reasoning, $D_a(v)$ must be a positive increasing function for $0 < v_{\text{imp}} \leq sv_0$. Since $v/P_a'(v) = 1/D_a(v) = (s/k_1)\omega(V)$, where $V = v/(sv_0)$, it is sufficient to show that $\omega(0) > 0$, $\omega(1) > 0$ and $\omega'(V) = 8(s-3)V + 3(8-3s) < 0$ for $0 < V \leq 1$. The first and the second inequalities are valid for $s > 2$ because $\omega(0) = 6(s-2) > 0$ and $\omega(1) = s > 0$. Since $\omega'(V)$ is a linear function, the third inequality is equivalent to the conditions $\omega'(0) = 3(8-3s) \leq 0$, $\omega'(1) = -s \leq 0$ and $\omega'(0) + \omega'(1) \neq 0$. Consequently, $s \geq 8/3$ are the permissible values for s.

In order to obtain the most convenient approximation we set $s = 8/3$ when $\alpha_1 = 0$. Then

$$D = \frac{m}{kk_1} \times \begin{cases} 1/(\gamma_0 - \gamma_2 v^2) & \text{if } v < v_*, \\ v & \text{if } v \geq v_*, \end{cases} \tag{28}$$

where

$$\begin{aligned} \gamma_0 &= \frac{2\alpha_0}{k_1} = \frac{6(s-2)}{s^2 v_0} = 0.01844, \\ \gamma_2 &= -\frac{4\alpha_2}{k_1} = \frac{4(3-s)}{s^4 v_0^3} = 0.929318 \cdot 10^{-6}, \\ v_* &= sv_0 = 81.33. \end{aligned} \tag{29}$$

The modified Young's approximation and the proposed approximation are compared in Figure 1. Inspection of Figure 1 shows that the difference between them is negligibly small.

We assume that Equation (28) for the drag force remains valid for motion of the penetrator with a variable mass.

We assume also that the mass of the impactor does not exceed $m \geq 27\,\text{kg}$ or $m \geq 182\,\text{kg}$ in the case of penetration into soil or rock and concrete, correspondingly. This restriction can be relaxed using a smoother approximation of the function $\theta(m)$.

4. Analytical investigation of the limiting case

In order to estimate the upper bound for increasing the DOP by using the jet thruster, let us consider the problem with the minimum number of constraints. In this version of the statement of the problem,

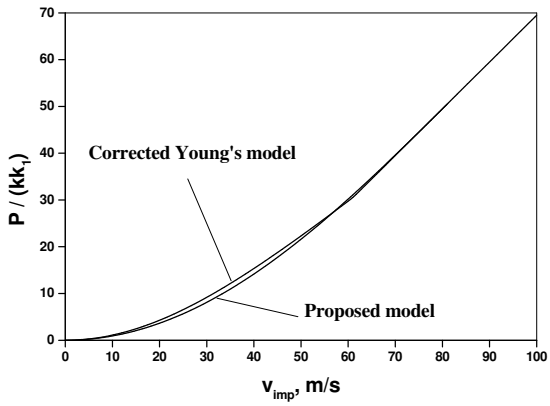

Figure 1. Comparison of the corrected Young's model and the proposed *smooth model*.

Equation (6) remains valid, and the constraints given by Equation (7), the first equation in Equation (11), and Equation (12) with $\mu_{\max} = \infty$, that is,

$$mv' + c \geq 0, \tag{30}$$

are taken into account.

We consider first penetration into nonfrozen soil, rock, or concrete. Then the formula for $\theta(m)$ in Equation (17) reads:

$$\theta(m) = \sigma m^{\kappa}, \qquad \kappa = \kappa_1 + \kappa_2, \tag{31}$$

where the values κ_1, κ_2, and σ are presented in Table 1. We assume that m varies in the range where σ is constant.

Using Equations (16) and (31), Equation (28) can be written as follows:

$$D = \frac{m^{1-\kappa}}{\sigma k_0 k_1} \times \begin{cases} 1/(\gamma_0 - \gamma_2 v^2) & \text{if } v < v_*, \\ v & \text{if } v \geq v_*. \end{cases} \tag{32}$$

Using the results of [Cicala and Miele 1956] (see also [Miele 1962]) the optimum curve must consist of the following subarcs:

subarc 1: $\Omega(m, v) = 0$, where

$$\Omega(m, v) = (v - c)D(m, v) + v(cdD/dv - mdD/dm), \tag{33}$$

subarc 2: the subarc $m = \text{const}$, and

subarc 3: the subarc $\dot{m} = -\mu_{\max}$ where $\dot{m} = dm/dt$.

Subarc 1 represents the solution of the Euler–Lagrange equation; subarc 3 is described by Equation (30) after replacing $\geq$ by $=$.

The above subarcs can be joined in the following sequences:

(a) if $\Omega > 0$ in some point then the only sequence $m = \text{const} \Rightarrow \dot{m} = -\mu_{\max}$ is possible in this point;

(b) if $\Omega < 0$ then the inverse sequence $\dot{m} = -\mu_{\max} \Rightarrow m = \text{const}$ is permissible;

(c) if $\Omega = 0$ then the joints $\Omega = 0 \Leftrightarrow \bar{m} = \text{const}$ and $\Omega = 0 \Leftrightarrow \dot{m} = -\mu_{\max}$ are possible.

The arrows indicate the direction of the motion of the penetrator along the subarcs on the m, v plane. Substituting D from Equation (32) into Equation (33), we obtain:

$$\Omega = \frac{\kappa m^{1-\kappa}}{\sigma k_0 k_1} \times \begin{cases} -\gamma_2(\gamma_0 - \gamma_2 v^2)^{-2}\Omega_a(v) & \text{if } v < v_*, \\ \Omega_b(v) & \text{if } v \geq v_*, \end{cases} \tag{34}$$

where

$$\Omega_a(v) = v^3 - 3\hat{c}v^2 - \hat{\gamma}_0 v + \hat{\gamma}_0 \hat{c}, \tag{35}$$

with $\Omega_b(v) = v^2$, $\hat{c} = c/\kappa$, and $\hat{\gamma}_0 = \gamma_0/\gamma_2$. Since

$$\begin{aligned} &\Omega_a(-\infty) < 0, && \Omega_a(0) > 0, \\ &\Omega_a(v_*) = -\Omega_b(v_*)(\gamma_0 - \gamma_2 v^2)^2/\gamma_2 < 0, && \Omega_a(+\infty) > 0, \end{aligned} \tag{36}$$

the cubic equation $\Omega_a(v) = 0$ has 3 real roots, but only one root, $v_\times$, is located between 0 and v_*:

$$v_\times = \hat{c} + 2\left(\frac{\hat{\gamma}_0 + 3\hat{c}^2}{3}\right)^{1/2} \cos\left(\frac{\zeta}{3} + \frac{4\pi}{3}\right), \qquad \zeta = \cos^{-1}\left(\frac{3\hat{c}^2}{\hat{\gamma}_0 + 3\hat{c}^2}\right)^{3/2}. \tag{37}$$

The dependence $v_\times$ versus $\hat{c} = c/\kappa$ is shown in Figure 2.

Taking into account this result, and that $\Omega_b(v) > 0$ for $v \geq v_*$, we conclude that $\Omega(v) < 0$ when $0 \leq v < v_\times$, $\Omega(v_\times) = 0$, and $\Omega(v) > 0$ when $v > v_\times$. Therefore, the conditions $\Omega(v) < 0$, $\Omega(v) = 0$, and $\Omega(v) > 0$ correspond to the conditions $\bar{v} < \bar{v}_\times$, $\bar{v} = \bar{v}_\times$, and $\bar{v} > \bar{v}_\times$, respectively.

The equation of the arc 1 reads:

$$v = v_\times. \tag{38}$$

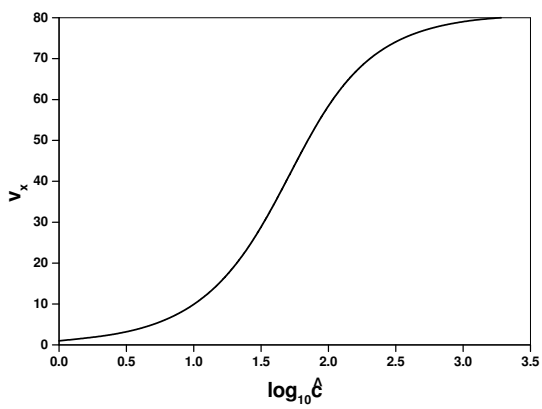

Figure 2. Solution of the equation $\Omega(v) = 0$ as a function of the parameter $\hat{c} = c\kappa$.

Consider a point moving along the curve $v = v_\times$, from the location with coordinates $(m_b, v_\times)$ to the location with coordinates $(m_a, v_\times)$, where $m_{\text{res}} \le m_a < m_b \le m_{\text{imp}}$. Then the increase of the functional given by Equation (6) with D determined by Equation (32) along this path reads:

$$\Delta H/(k_0k_1) = \Gamma_m(m_a, m_b) = cv_\times(\gamma_0 - \gamma_2 v_\times^2)\int_{m_a}^{m_b} \frac{dm}{m^{1-\kappa}} = c\hat{v}_\times(\gamma_0 - \gamma_2 v_\times^2)(m_b^\kappa - m_a^\kappa). \tag{39}$$

Along the line $v = v_\times < v_*$, Equation (1) reads:

$$c\frac{dm}{dt} = -\frac{m^{1-\kappa}}{k_0k_1(\gamma_0 - \gamma_2 v_\times^2)}. \tag{40}$$

The solution to Equation (40) with the initial conditions $m(t_b) = m_b$ is as follows:

$$m = [m_b^\kappa - \tau(t - t_b)]^{1/\kappa}, \qquad \tau = \frac{\kappa}{ck_0k_1(\gamma_0 - \gamma_2 v_\times^2)}. \tag{41}$$

Increase of the mass of the penetrator from m_b to m_a occurs up to the time $t = t_a$ where $t_a = t_b + (m_b^\kappa - m_a^\kappa)/\tau$.

Subarc 2 corresponds to the motion with a constant mass. Assume that the velocity of the impactor decreases from $v = v_b$ to $v = v_a$ while its mass remains constant, $m = m_0$. Then the increase of the functional given by Equation (6) is as follows:

$$\begin{aligned}\Delta H/(k_0k_1) &= \Gamma_v^{(1)}(m_0, v_a, v_b)\\ &= m_0^\kappa \int_{v_a}^{v_b} v(\gamma_0 - \gamma_2 v^2)dv\\ &= 0.25m_0^\kappa(v_b^2 - v_a^2)[2\gamma_0 - \gamma_2(v_b^2 + v_a^2)] \quad \text{if } v_b \le v_\times,\end{aligned} \tag{42}$$

and

$$\Delta H/(k_0k_1) = \Gamma_v^{(2)}(m_0, v_a, v_b) = m_0^\kappa \int_{v_a}^{v_b} dv = m_0^\kappa(v_b - v_a) \qquad \text{if } v_b \ge v_\times. \tag{43}$$

Along subarc 3, $\dot{m} = -\mu_{\max} = -\infty$. The equation of this subarc in the coordinates (m, v) is determined by Equation (30) after replacing $\ge$ by $=$:

$$mv + c = 0. \tag{44}$$

The solution of this ODE with separable variables passing through the point (m_{imp}, v_0) can be written as follows:

$$v = v_0 - c\ln(m/m_{\text{imp}}). \tag{45}$$

This trajectory corresponds to the step change of the mass of the penetrator (the pulse burning). This change of the mass and of the velocity of the penetrator occurs without change of its location.

Analysis of the conditions presented at the beginning of this section shows that three versions of burning program (BP) are possible, depending on the values of the parameters $\hat{c}$ and v_{imp}.

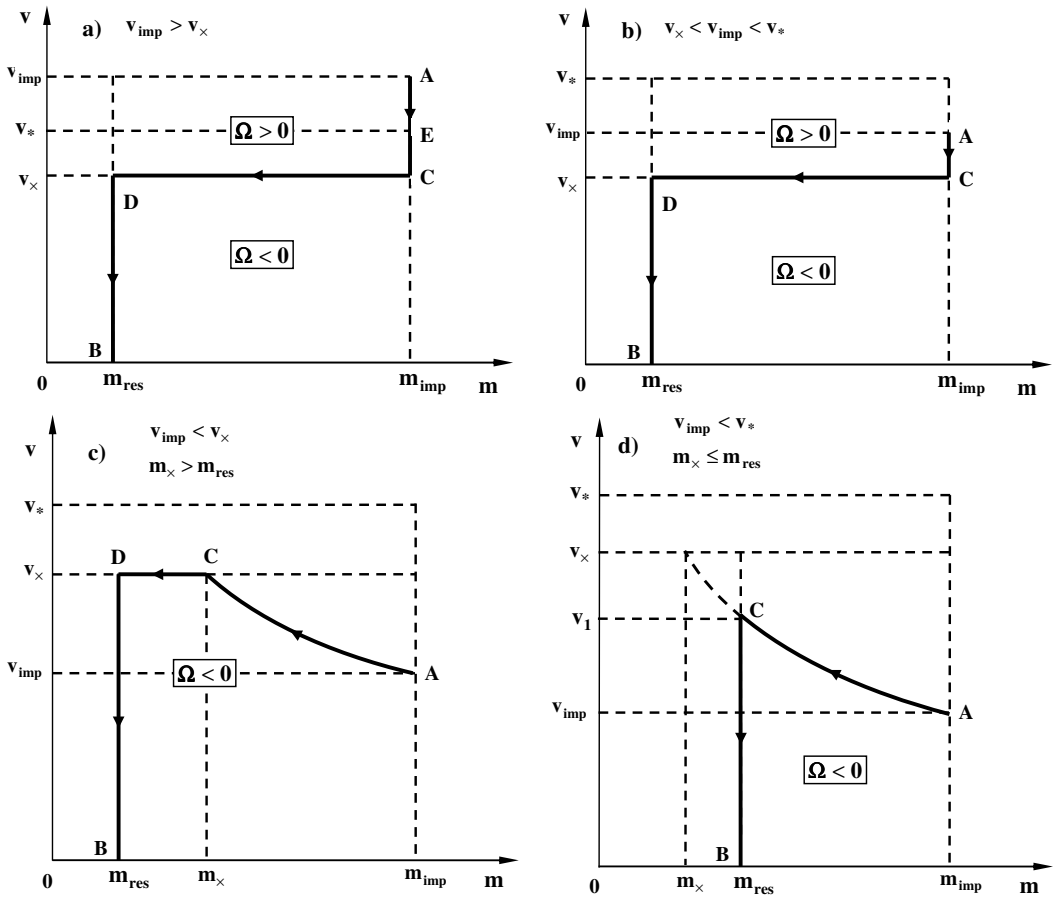

Figure 3. Stages of optimal burning programs for penetration into nonfrozen soil, rock, and concrete shields, $\bar{\beta}_{\min} = 0$.

Consider the case when $v_{\text{imp}} > v_*$. Taking into account that $v_* > v_\times$, the optimal BP includes the following subarcs (Figure 3a) in the coordinates (m, v):

$$\begin{cases} AE : m = m_{\text{imp}}, & v : v_{\text{imp}} \to v_*, \\ EC : m = m_{\text{imp}}, & v : v_* \to v_\times, \\ CD : v = v_\times, & m : m_{\text{imp}} \to m_{\text{res}}, \\ DB : m = m_{\text{res}}, & v : v_\times \to 0. \end{cases} \tag{46}$$

The corresponding expression for the DOP reads:

$$H/(k_0 k_1 m_{\text{imp}}^{\kappa}) = \Gamma_v^{(2)}(1, v_*, v_{\text{imp}}) + \Gamma_v^{(1)}(1, v_\times, v_*) + \Gamma_m(\bar{m}_{\text{res}}, 1) + \Gamma_v^{(1)}(\bar{m}_{\text{res}}, 0, v_\times), \tag{47}$$

with $\bar{m}_{\text{res}} = m_{\text{res}}/m_{\text{imp}}$. In the case $v_{\text{imp}} = v_*$, the segment AE vanishes.

If $v_\times < v_{\text{imp}} < v_*$, then the optimal BP includes the subarcs (Figure 3b):

$$\begin{cases} AC : m = m_{\text{imp}}, & v : v_{\text{imp}} \to v_\times, \\ CD : v = v_\times, & m : m_{\text{imp}} \to m_{\text{res}}, \\ DB : m = m_{\text{res}}, & v : v_\times \to 0, \end{cases} \tag{48}$$

and the DOP is as follows:

$$H/(k_0 k_1 m_{\text{imp}}^\kappa) = \Gamma_v^{(1)}(1, v_\times, v_{\text{imp}}) + \Gamma_m(\bar{m}_{\text{res}}, 1) + \Gamma_v^{(1)}(\bar{m}_{\text{res}}, 0, v_\times). \tag{49}$$

In the case $v_{\text{imp}} = v_\times$, the segment AC vanishes.

Motion of a penetrator which is described by Equations (46) and (48) includes (in a general case) the following stages: *passive* penetration when a jet thruster is turned off until the velocity slows down to the magnitude $v_\times$ (segment AC of the trajectory), motion with a constant velocity $v_\times$ with an operating jet thruster until complete exhaustion of fuel supply (segment CD of the trajectory), and passive penetration until a penetrator slows down to zero velocity (segment DB of the trajectory).

Consider now the case when $v_{\text{imp}} < v_\times$ and the curve determined by Equation (45) with $v_0 = v_{\text{imp}}$ intersects with the line $v = v_\times$ in the point $(m_\times, v_\times)$, where $m_\times > m_{\text{res}}$ (Figure 3c). Then the optimal BP includes three subarcs:

$$\begin{cases} AC : v = v_0 - c\ln(m/m_{\text{res}}), & m : m_{\text{imp}} \to m_\times, \\ CD : v = v_\times, & m : m_\times \to m_{\text{res}}, \\ DB : m = m_{\text{res}}, & v : v_\times \to 0, \end{cases} \tag{50}$$

where $m_\times = m_{\text{imp}} \exp((1 - v_\times)/c)$.

Equation (50) describes the following stages of the controlled motion of a penetrator: operation of a jet thruster in the impulse regime whereby the penetrator's velocity instantaneously changes from the initial value, v_{imp}, to $v_\times$ by spending a mass of fuel equal to $m_{\text{imp}} - m_\times$ without the motion of a penetrator (subarc AC); operation of a jet thruster for providing a constant velocity to the penetrator, $v_\times$, until exhaustion of the fuel supply (segment CD); and passive penetration until a penetrator slows down to zero velocity (segment DB of the trajectory).

The corresponding expression for the DOP is as follows:

$$H/(k_0 k_1 m_{\text{imp}}^\kappa) = \Gamma_m(\bar{m}_{\text{res}}, \bar{m}_\times) + \Gamma_v^{(1)}(\bar{m}_{\text{res}}, 0, v_\times), \tag{51}$$

with $\bar{m}_\times = m_\times / m_{\text{imp}}$.

If $v_{\text{imp}} < v_\times$ and $m_\times \le m_{\text{res}}$ then the optimal BP includes two subarcs (Figure 3d):

$$\begin{cases} AC : v = v_0 - c\ln(m/m_{\text{res}}), & m : m_{\text{imp}} \to m_{\text{res}}, \\ CB : m = m_{\text{res}}, & v : v_1 \to 0, \end{cases} \tag{52}$$

where $v_1 = v_{\text{imp}} - c\ln \bar{m}_{\text{res}}$.

Here, a jet thruster operates in the impulse regime until exhausting the whole fuel supply. In this case the velocity of the penetrator instantaneously changes from the initial velocity to v_1 (segment AC of the trajectory). Afterwards, this penetrator continues its motion until it slows down to zero velocity (segment CB of the trajectory).

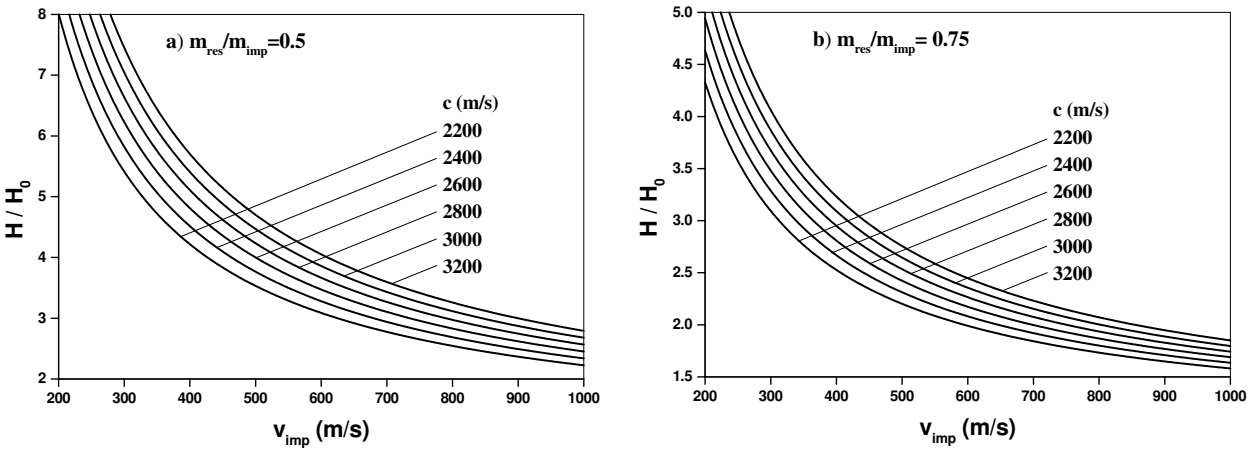

Figure 4. Normalized optimal DOP into nonfrozen soil, rock, and concrete shields versus impact velocity; H is DOP for the optimal burning program, H_0 is DOP for a passive trajectory, $\bar{\beta}_{\min} = 0$, $\kappa = 0.7$.

The DOP is determined using only the subarc CB:

$$H/(k_0 k_1 m_{\text{imp}}^{\kappa}) = \Gamma_v^{(1)}(\bar{m}_{\text{res}}, 0, v_1). \tag{53}$$

The depth of passive penetration of the impactor with the mass m_{imp} is as follows:

$$\frac{H_0}{k_0 k_1 m_{\text{imp}}^{\kappa}} = \begin{cases} \Gamma_v^{(1)}(1, 0, v_{\text{imp}}) & \text{if } v_{\text{imp}} \le v_*, \\ \Gamma_v^{(2)}(1, v_*, v_{\text{imp}}) + \Gamma_v^{(1)}(1, 0, v_*), & \text{if } v_{\text{imp}} > v_*. \end{cases} \tag{54}$$

Some of the above relationships can be simplified by taking into account that $v_\times \approx v_*$ for $c > 2000$ m/s (Figure 2).

We use the ratio

$$\eta = H/H_0, \tag{55}$$

which depends on v_{imp}, c, $\bar{m}_{\text{res}}$, and κ, for comparing the DOP with the optimal BP and the depth of passive penetration (Figure 4). Although η can attain very large values for relatively small impact velocities, the absolute values of the DOP, H, are reasonable. The results for the relatively high impact velocities are the most interesting because of the feasibility for increasing the absolute DOP by using the jet thruster.

The optimum BP for the impact velocities, $v_{\text{imp}} > v_* \approx 81$ m/s, is simple: passive penetration up to velocity $v_\times$, motion with constant velocity $v_\times$ while the propellant is available (the consumption of the propellant is described by Equation (41)) with $m_a = m_{\text{res}}$ and $m_b = m_{\text{imp}}$, $m = [m_{\text{res}}^{\kappa} - \tau(t - t_{\text{res}})]^{1/\kappa})$, and passive penetration until rest. This BP is valid if the constraints on mass fluxes and penetrator's acceleration are not taken into account. Let us determine the conditions under which these constraints do not affect this optimum BP.

The constraints given by Equation (3) are relevant only on the path of the trajectory where $v = v_\times$. Equation (1) implies that $dm/dt = -D(m, v_\times)/c = -(\tau/\kappa)m^{1-\kappa}$. Substituting this relationship into

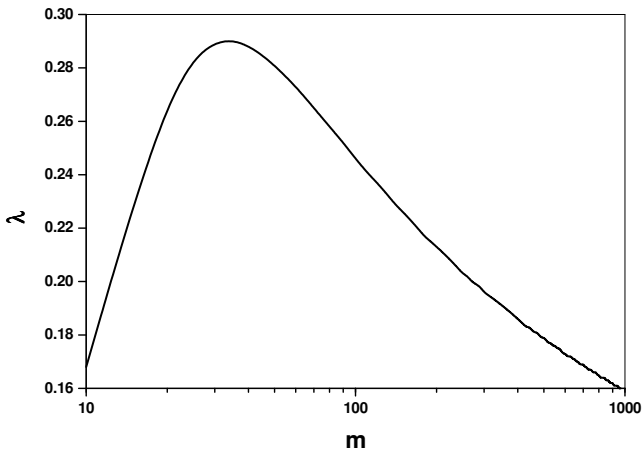

Figure 5. Dependence $\lambda = \lambda(m)$ in the model of penetration into ice and frozen soil.

Equation (3) we obtain the inequality $m \le (\kappa\mu_{\max}/\tau)^{1/(1-\kappa)}$ that must be satisfied for $m_{\text{res}} \le m \le m_{\text{imp}}$. Since the mass decreases on this interval, the above inequality can be substituted by the following:

$$m_{\text{imp}} \le (\kappa\mu_{\max}/\tau)^{1/(1-\kappa)}. \tag{56}$$

The constraints given by Equation (3) are relevant only on the segment of the trajectory with a constant mass, $m = \tilde{m}$. Equation (1) implies that $dv/dt = -D(\tilde{m}, v)/\tilde{m}$. Substituting this relationship into Equation (3) we obtain:

$$D(m_{\text{imp}}, v) \le m_{\text{imp}} g\chi_{\max} \qquad \text{if } v_\times \le v \le v_{\text{imp}},$$
$$D(m_{\text{res}}, v) \le m_{\text{res}} g\chi_{\max} \qquad \text{if } 0 \le v \le v_\times.$$

Since D is an increasing function of v, these constraints are valid if

$$D(m_{\text{imp}}, v_{\text{imp}}) \le m_{\text{imp}} g\chi_{\max} \qquad \text{and} \qquad D(m_{\text{res}}, v_\times) \le m_{\text{res}} g\chi_{\max}.$$

The two latter inequalities imply that

$$m_{\text{imp}} \ge \frac{v_{\text{imp}}}{k_0 k_1 g\chi_{\max}}, \qquad m_{\text{res}} \ge \frac{1}{k_0 k_1 (\gamma_0 - \gamma_2 v_\times^2) g\chi_{\max}}. \tag{57}$$

Let us consider the case of penetration into ice and frozen soil shields. Then

$$\theta(m) = m^{0.6} \ln(50 + 0.29m^2)$$

and

$$D = \frac{m^{0.4}}{k_0 k_1 \ln(50 + 0.29m^2)} \times \begin{cases} 1/(\gamma_0 - \gamma_2 v^2) & \text{if } v < v_*, \\ v & \text{if } v \ge v_*. \end{cases} \tag{58}$$

Substituting D from this equation into Equation (33) we obtain:

$$\Omega = \frac{m^{0.4}[0.6+\lambda(m)]}{k_0 k_1 \ln(50+0.29m^2)} \times \begin{cases} -\gamma_2(\gamma_0-\gamma_2 v^2)^{-2}\Omega_a(v) & \text{if } v < v_*, \\ \Omega_b(v) & \text{if } v \geq v_*, \end{cases} \tag{59}$$

where

$$\begin{gathered} \Omega_a(m,v) = v^3 - 3\hat{c}v^2 - \hat{\gamma}_0 v + \hat{\gamma}_0\hat{c}, \\ \Omega_b(v) = v^2, \qquad \hat{\gamma}_0 = \gamma_0/\gamma_2, \\ \hat{c} = \frac{c}{0.6+\lambda(m)}, \qquad \lambda(m) = \frac{0.58m^2}{(50+0.29m^2)\ln(50+0.29m^2)}. \end{gathered} \tag{60}$$

The equation $\Omega(m,v)=0$ determines the subarc $v = v_\times(m)$ where $v_\times(m)$ is determined by Equation (37) with $\hat{c} = \hat{c}(m)$ from Equation (60). In contrast to the case of SRC shields, the subarc is curvilinear in this case.

Let us investigate now the behavior of the function $\lambda(m)$. Changing the variable $50+0.29m^2 = x$ we reduce the problem to analyzing the function

$$\Theta(x) = \lambda\left(\sqrt{\frac{x-50}{0.29}}\right) = \frac{2(x-50)}{x\ln x}. \tag{61}$$

Let us calculate the derivative:

$$\begin{aligned} \Theta'(x) &= \frac{2}{x\ln x}\Theta_0(x), \\ \Theta_0(x) &= 50(\ln x + 1) - x, \\ \Theta_0'(x) &= \frac{50}{x} - 1. \end{aligned} \tag{62}$$

For $x > 50$, $\Theta_0'(x) < 0$. Hence, $\Theta_0(x)$ decreases in this semiinfinite interval. Since $\Theta_0(50) > 0$ and $\Theta_0(350) < 0$ we conclude that the equation $\Theta_0(x) = 0$ has a single root which can be easily determined, $x = x_0 \approx 341.7$. This point is the maximum of the function $\Theta(x)$ that increases from $\Theta(50) = 0$ to $\Theta(x_0) \approx 0.293$ and then decreases to 0. Therefore, $0 < \lambda(m) \leq 0.293$, and the maximum is attained for $m = m_0 \approx 31.7$ kg (Figure 5). Equation (60) shows that $1.12c < \hat{c} \leq 1.67c$ and, for $c > 2000$ m/s, the value $v_\times$ is very close to v_* and practically does not vary (Figure 2). Consequently, the subarc which is determined by equation $\Omega(m,v) = 0$ is only slightly different from a straight line. Therefore, the trajectory which is close to the optimum for all considered shield materials is the following ($v_{\text{imp}} > v_* \approx 81$ m/s): passive penetration until to velocity v_* is attained, motion with a constant velocity v_* while the propellant is available, and passive penetration until rest. The analysis shows that the effect of the material of the shield on the coefficient η is insignificant.

5. Application of dynamic programming for numerical investigation of the problem

Equations (6), (7), (10), (11), (12), and (13) describe the variational problem considered here in the general case, and imply the following expressions which can be written using, for convenience, the

dimensionless variables that are defined below:

$$\bar{H} = \int_{\bar{m}_{\text{res}}}^{1} \frac{(\bar{m}\bar{v}' + \bar{c})\bar{v}}{\bar{D}(\bar{m}, \bar{v})} d\bar{m}, \tag{63}$$

$$\bar{v}(1) = 1, \qquad \bar{v}(\bar{m}_{\text{res}}) = 0, \qquad 0 \le \bar{v}(\bar{m}) \le v_{\max}, \qquad \bar{m}_{\text{res}} \le \bar{m} \le 1, \tag{64}$$

$$\bar{m}\bar{v}' + \bar{c} \ge \bar{\beta}_{\min}\bar{D}(\bar{m}, \bar{v}) \qquad \text{if } \bar{v}' < \infty, \tag{65}$$

$$\left| \frac{\bar{D}(\bar{m}, \bar{v})\bar{v}'}{\bar{m}\bar{v}' + \bar{c}} \right| \le \bar{\chi}_{\max} \qquad \text{if } \bar{v}' < \infty, \tag{66}$$

$$D(\bar{m}, \bar{v})/\bar{m} \le \bar{\chi}_{\max} \qquad \text{if } \bar{m} = \text{const}, \tag{67}$$

where

$$\bar{v} = \frac{v}{v_{\text{imp}}}, \qquad \bar{c} = \frac{c}{v_{\text{imp}}}, \qquad \bar{v}_{\max} = \frac{v_{\max}}{v_{\text{imp}}}, \qquad \bar{m}_{\text{res}} = \frac{m_{\text{res}}}{m_{\text{imp}}},$$

$$\bar{m} = \frac{m}{m_{\text{imp}}}, \qquad \bar{\beta}_{\min} = \frac{v_{\text{imp}} m_{\text{imp}}}{L\mu_{\max}}, \qquad \bar{\chi}_{\max} = \frac{Lg\chi_{\max}}{v_{\text{imp}}^2}, \qquad \bar{h} = \frac{h}{L},$$

$$\bar{H} = \frac{H}{L}, \qquad \bar{v}' = \frac{d\bar{v}}{d\bar{m}},$$

$$\bar{D}(\bar{m}, \bar{v}) = \frac{L}{v_{\text{imp}}^2 m_{\text{imp}}} D(m_{\text{imp}}\bar{m}, v_{\text{imp}}\bar{v}), \tag{68}$$

and L is some characteristic length.

The problem is reduced to the optimization of the functional $\bar{H}$ in Equation (63), whereas the solution must satisfy the constraints given by Equations (64)–(66).

Dynamic programming for the general model of a drag force. Dynamic programming is an appropriate method for determining the optimal BP. Note that optimization of the flight of an aircraft with a jet engine was mentioned in one of the first books on dynamic programming [Bellman et al. 1958] as an example of a possible application of dynamic programming. This method allows determining a global extremum while taking into account constraints. In the following, we describe an application of dynamic programming to the above formulated optimization problem that has some characteristic properties.

In order to solve the variational problem for the functional given by Equation (63), the function $\bar{v}(\bar{m})$ can be approximated as a piecewise linear function determined by the values (Figure 6)

$$\bar{v}^{(0)} = 0, \qquad \bar{v}^{(1)}, \ldots, \bar{v}^{(j)}, \ldots, \bar{v}^{(N_m - 1)}, \qquad \bar{v}^{(N_m)}$$

$$\bar{w}^{(0)}, \qquad \bar{w}^{(1)}, \ldots, \bar{w}^{(j)}, \ldots, \bar{w}^{(N_m - 1)}, \qquad \bar{w}^{(N_m)} = 1$$

in $N_m + 1$ equally spaced mesh points of interpolation

$$\bar{m}^{(0)} = \bar{m}_{\text{res}}, \bar{m}^{(1)}, \ldots, \bar{m}^{(j)}, \ldots, \bar{m}^{(N_m - 1)}, \qquad \bar{m}^{(N_m)} = 1,$$

where $\bar{m}^{(j)} = \bar{m}_{\text{res}} + j\Delta\bar{m}$, $\Delta\bar{m} = (1 - \bar{m}_{\text{res}})/N_m$, $j = 0, 1, 2, \ldots, N_m$. The unknown values of the function, $\bar{v}^{(j)}$ and $\bar{w}^{(j)}$ are chosen among the finite set of values $0, \Delta\bar{v}, 2\Delta\bar{v}, \ldots, N_v\,\Delta\bar{v}$, where $\Delta\bar{v} =$

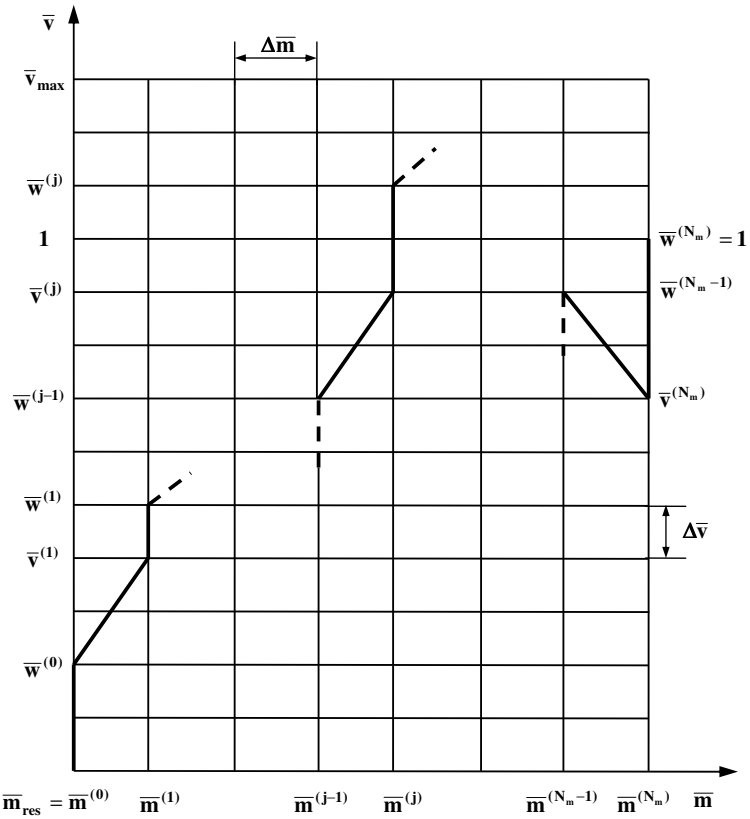

Figure 6. Discretization of the problem.

$\bar{v}_{\max}/N_v$ and $v_{\max}$ is a given upper bound for the velocity of the penetrator. Penetration of the impactor is associated with the trajectory

$$(\bar{m}^{(N_m)}, \bar{w}^{(N_m)}) \to (\bar{m}^{(N_m)}, \bar{v}^{(N_m)}) \to (\bar{m}^{(N_m-1)}, \bar{w}^{(N_m-1)}) \to (\bar{m}^{(N_m-1)}, \bar{v}^{(N_m-1)}) \to \cdots$$
$$\to (\bar{m}^{(1)}, \bar{w}^{(1)}) \to (\bar{m}^{(1)}, \bar{v}^{(1)}) \to (\bar{m}^{(0)}, \bar{w}^{(0)}) \to (\bar{m}^{(0)}, \bar{v}^{(0)}).$$

Since the velocity of the impactor cannot increase without burning fuel, $\bar{v}^{(j)} \le \bar{w}^{(j)}$ for all j.

The equation of the straight line between the points $(\bar{m}^{(j-1)}, \bar{w}^{(j-1)})$ and $(\bar{m}^{(j)}, \bar{v}^{(j)})$ can be written as follows:

$$\bar{v} = e^{(j)}\bar{m} + f^{(j)}, \qquad e^{(j)} = \frac{\bar{v}^{(j)} - \bar{w}^{(j-1)}}{\bar{m}^{(j)} - \bar{m}^{(j-1)}},$$
$$f^{(j)} = \frac{\bar{m}^{(j)}\bar{w}^{(j-1)} - \bar{m}^{(j-1)}\bar{v}^{(j)}}{\bar{m}^{(j)} - \bar{m}^{(j-1)}}, \tag{69}$$

$j = 1, 2, \ldots, N_m$. Then the integral in Equation (63) along the piecewise linear contour can be written as follows:

$$\bar{H} = Q_v^{(0)} + \sum_{j=1}^{N_m} (Q_m^{(j)} + Q_v^{(j)}), \tag{70}$$

where $Q_m^{(j)}$ and $Q_v^{(j)}$ are the components of the integral over *vertical* and *nonvertical* segments of the trajectory, correspondingly (Figure 6),

$$\begin{aligned} Q_v^{(j)} &= \int_{\bar{v}^{(j)}}^{\bar{w}^{(j)}} G_v^{(j)}(\bar{v}) d\bar{v}, \\ G_v^{(j)}(\bar{v}) &= \frac{\bar{m}^{(j)}\bar{v}}{\bar{D}(\bar{m}^{(j)}, \bar{v})}, \qquad j = 0, 1, 2, \ldots, N_m, \end{aligned} \tag{71}$$

$$\begin{aligned} Q_m^{(j)} &= \int_{\bar{m}^{(j-1)}}^{\bar{m}^{(j)}} G_m^{(j)}(\bar{m}) d\bar{m}, \\ G_m^{(j)}(\bar{m}) &= \frac{(e^{(j)}\bar{m} + \bar{c})(e^{(j)}\bar{m} + f^{(j)})}{\bar{D}(\bar{m}, e^{(j)}\bar{m} + f^{(j)})}, \qquad j = 1, 2, \ldots, N_m. \end{aligned} \tag{72}$$

Integrals in Equation (71) can be often calculated in explicit form. Otherwise, one can use, for instance, the trapezoid rule formula with points of interpolation, $\bar{v}_\xi^{(j)}$, in nodes of the $(\bar{m}, \bar{v})$ mesh. Then

$$Q_v^{(j)}/\Delta\bar{v} = 0.5\big[G_v^{(j)}(\bar{v}_0^{(j)}) + G_v^{(j)}\big(\bar{v}_{n_v^{(j)}}^{(j)}\big)\big] + \sum_{\substack{\xi=1 \\ n_v^{(j)}>1}}^{n_v^{(j)}-1} G_v^{(j)}\big(\bar{v}_\xi^{(j)}\big), \tag{73}$$

where $n_v^{(j)}$ is the integral part $(\bar{w}^{(j)} - \bar{v}^{(j)})/\Delta\bar{v}$ and

$$\bar{v}_\xi^{(j)} = \bar{v}^{(j)} + \xi\Delta\bar{v}, \qquad \xi = 0, 1, \ldots, n_v^{(j)}. \tag{74}$$

In a similar manner, integrals in Equation (72) can be represented as

$$Q_m^{(j)}/\Delta\bar{m}^{(j)} = 0.5\big[G_m^{(j)}(\bar{m}_0^{(j)}) + G_m^{(j)}\big(\bar{v}_{n_m^{(j)}}^{(j)}\big)\big] + \sum_{\substack{\xi=1 \\ n_m^{(j)}>1}}^{n_m^{(j)}-1} G_m^{(j)}\big(\bar{v}_\xi^{(j)}\big), \tag{75}$$

where $n_m^{(j)} + 1$ is the selected number of points of interpolations at the interval $[\bar{m}^{(j-1)}, \bar{m}^{(j)}]$,

$$\bar{m}_\xi^{(j)} = m^{(j)} + \xi\Delta\bar{m}^{(j)}, \qquad \xi = 0, 1, \ldots, n_m^{(j)}, \qquad \Delta\bar{m}^{(j)} = \Delta m/n_m^{(j)}. \tag{76}$$

Inequalities in Equations (65) and (66) can be written in the points of interpolations in the following form:

$$A_\xi^{(j)} \geq \bar{\beta}_{\min}, \qquad |e^{(j)}| \leq \bar{\chi}_{\max}|A_\xi^{(j)}|, \tag{77}$$

where

$$A_\xi^{(j)} = \frac{e^{(j)}\bar{m}_\xi^{(j)} + \bar{c}}{\bar{D}(\bar{m}_\xi^{(j)}, e^{(j)}\bar{m}_\xi^{(j)} + f^{(j)})}, \qquad j = 1, 2, \ldots, N_m,\ \xi = 0, 1, \ldots, n_m^{(j)}. \tag{78}$$

Inequality (67) implies the following constraints:

$$\bar{D}(\bar{m}^{(j)}, \bar{v}_\xi^{(j)})/\bar{m}^{(j)} \le \bar{\chi}_{\max}, \qquad j = 1, 2, \ldots, N_m,\ \xi = 0, 1, \ldots, n_v^{(j)}. \tag{79}$$

We do not allow regimes whereby fuel is exhausted while the velocity of the penetrator remains zero, that is, the following condition must be satisfied:

$$\bar{v}^{(j)} + \bar{w}^{(j-1)} > 0, \qquad j = 1, 2, \ldots, N_m. \tag{80}$$

Unlike the standard approach (see, for example, [Pedregal 2003]), we allow *vertical* segments in the optimal curve, use a more accurate approximation of the criterion on the subintervals, and take into account the constraints in the intermediate points of the subintervals. The second factor enhances the reliability of the analysis.

The case of the generalized Young's penetration model. In the case of the generalized Young model we obtain:

$$\bar{D}(\bar{m}, \bar{v}) = \frac{L\psi(\bar{v})}{k_0 k_1 v_{\text{imp}}^2 \varphi(\bar{m})}, \tag{81}$$

where

$$\psi(\bar{v}) = \begin{cases} 1/(\gamma_0 - \gamma_2 v_{\text{imp}}^2 \bar{v}^2) & \text{if } \bar{v} < \bar{v}_*, \\ v_{\text{imp}}\bar{v} & \text{if } \bar{v} \ge \bar{v}_*, \end{cases} \tag{82}$$

$$\varphi(\bar{m}) = \begin{cases} \sigma m_{\text{imp}}^{\gamma_1+\gamma_2} \bar{m}^{\gamma_1+\gamma_2-1} & \text{if SRC}, \\ m_{\text{imp}}^{\gamma_1} \bar{m}^{\gamma_1-1} \ln(50 + 0.29 m_{\text{imp}}^2 \bar{m}^2) & \text{if IFS}, \end{cases} \tag{83}$$

$\bar{v}_* = v_*/v_{\text{imp}}$, and it is assumed that the substitution $m = m_{\text{imp}}\bar{m}$ is made in Table 1.

For the vertical segments of the trajectory, the analysis can be performed in the exact analytical form. Clearly, the integral in Equation (71) can be calculated:

$$Q_v^{(j)} = \frac{k_0 k_1 v_{\text{imp}}^2 \bar{m}^{(j)} \varphi(\bar{m}^{(j)})}{L} \int_{\bar{v}^{(j)}}^{\bar{w}^{(j)}} \frac{\bar{v}d\bar{v}}{\psi(\bar{v})}, \qquad j = 0, 1, 2, \ldots, N_m, \tag{84}$$

where

$$\int_{\bar{v}^{(j)}}^{\bar{w}^{(j)}} \frac{\bar{v}d\bar{v}}{\psi(\bar{v})} = \begin{cases} \Phi(\bar{v}^{(j)}, \bar{w}^{(j)}) & \text{if } \bar{w}^{(j)} < \bar{v}_*, \\ \Phi(\bar{v}^{(j)}, \bar{v}_*) + \Psi(\bar{v}_*, \bar{w}^{(j)}) & \text{if } \bar{v}^{(j)} \le \bar{v}_* \le \bar{w}^{(j)}, \\ \Psi(\bar{v}^{(j)}, \bar{w}^{(j)}) & \text{if } \bar{v}_* < \bar{v}^{(j)}, \end{cases} \tag{85}$$

$$\Phi(\bar{V}_a, \bar{V}_b,) = \int_{\bar{V}_a}^{\bar{V}_b} (\gamma_0 - \gamma_2 v_{\text{imp}}^2 \bar{v}^2)\bar{v} d\bar{v}$$
$$= 0.25(\bar{V}_b^2 - \bar{V}_a^2)\left[2\gamma_0 - \gamma_2 v_{\text{imp}}^2 (\bar{V}_b^2 + \bar{V}_a^2)\right], \tag{86}$$
$$\Psi(\bar{V}_a, \bar{V}_b) = \frac{1}{v_{\text{imp}}} \int_{\bar{V}_a}^{\bar{V}_b} d\bar{v} = (\bar{V}_b - \bar{V}_a)/v_{\text{imp}}.$$

Instead of Equation (79), the constraints in Equation (67) can be written as follows:

$$\bar{w}^{(j)} \le \psi^{-1}\left(\frac{k_0 k_1 v_{\text{imp}}^2 \bar{m}^{(j)} \varphi(\bar{m}^{(j)}) \bar{\chi}_{\max}}{L}\right), \qquad j = 0, 1, 2, \ldots, N_m, \tag{87}$$

where

$$\psi^{-1}(z) = \begin{cases} \sqrt{\dfrac{\gamma_0 z - 1}{\gamma_2 v_{\text{imp}}^2 z}} & \text{if } z \le v_{\text{imp}} \bar{v}_*, \\ z/v_{\text{imp}} & \text{if } z > v_{\text{imp}} \bar{v}_*, \end{cases} \tag{88}$$

6. Results of numerical optimization

Figure 7 shows typical results of calculations for which we selected the following data: penetration into nonfrozen soil, rock, and concrete shields, $m_{\text{imp}} = 400$ kg, $m_{\text{res}} = 200$ kg, $v_{\text{imp}} = 700$ m/s $> v_*$, $\chi_{\max} = \infty$.

Figure 7a, b shows optimal BPs. For small values of $\bar{\beta}_{\min}$ when the constraint on the fuel flow rate is irrelevant, the regime of motion is as follows: inertial motion until velocity $\bar{v}_\times$ is attained; motion with a constant velocity $\bar{v}_\times$ until exhausting fuel supply, and, finally, inertial motion until rest. From some value, the effect of $\bar{\beta}_{\min}$ on the optimal BP becomes pronounced: the regime with a maximum fuel flow rate appears between the initial passive regime and the regime with a constant velocity $\bar{v}_\times$. Further increase of $\bar{\beta}_{\min}$ results in the following changes: transition from a passive penetration to the motion with the maximum fuel flow rate at larger velocities, the regime of motion with a constant velocity $\bar{v}_\times$ gradually vanishes, and the regime with the maximum fuel flow rate switches to the regime of inertial penetration with mass $\bar{m}_{\text{res}}$. From some magnitude of $\bar{\beta}_{\min}$, a solution does not exist. The latter means that the penetrator slows down to zero velocity before exhausting the fuel supply for any BP.

In Figure 7c, we showed the dependencies of the maximum normalized DOP, $\eta = H/H_0$, as a function of parameter $\bar{\beta}_{\min}$ for different values of the dimensionless relative exit velocity of gases at the nozzle of the thruster, c; clearly, H_0 is the same when the variants with different $\bar{\beta}_{\min}$ and c are compared. The maximum effect of using a jet thruster is observed for small $\bar{\beta}_{\min}$. An increase of $\bar{\beta}_{\min}$ implies stronger constraints, namely, reducing the upper bound for the admissible fuel consumption rate of the thruster. The curves $\eta = \eta(\bar{\beta}_{\min})$ are located higher, with an increase of c, that is, a negative effect of $\bar{\beta}_{\min}$ can be compensated by increasing c. The fact that some curves of the dependencies $\eta = \eta(\bar{\beta}_{\min})$ are terminated implies that the capabilities of the thruster are inadequate, and penetration terminates before exhausting fuel supply.

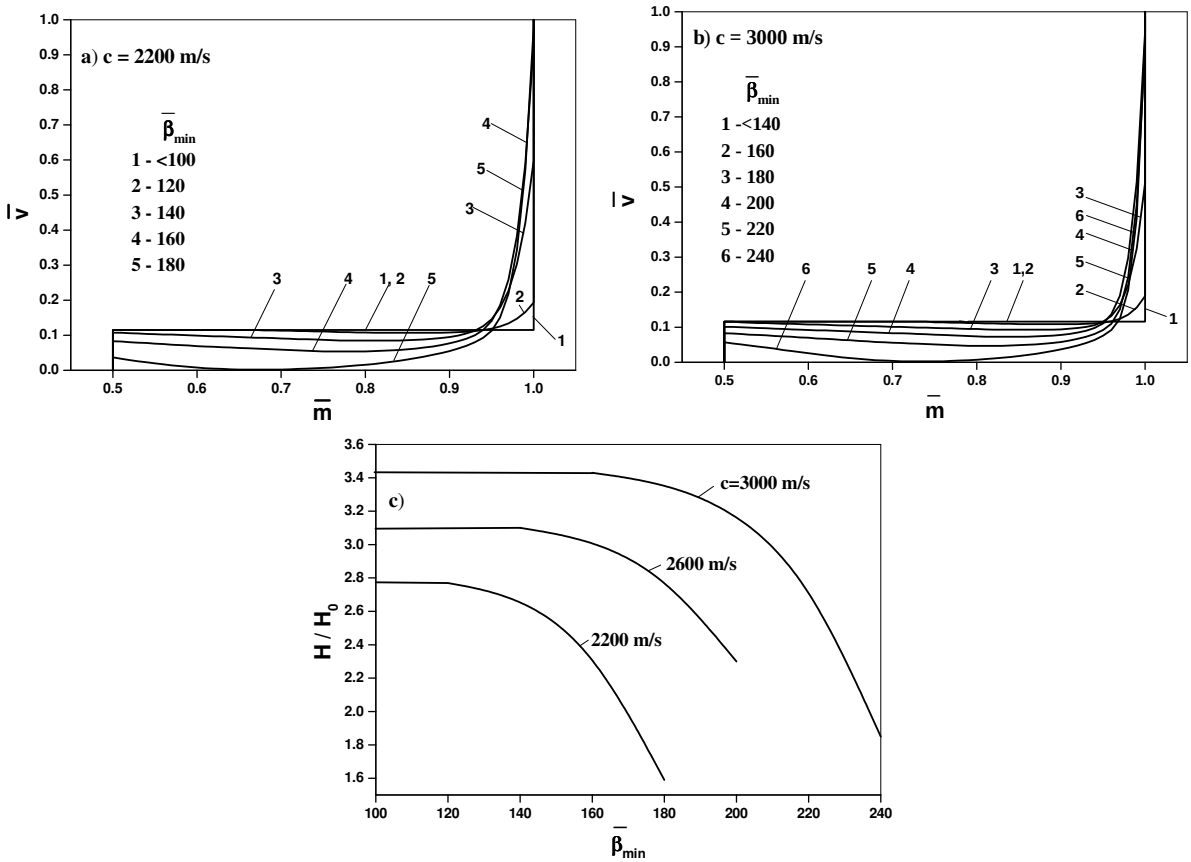

Figure 7. Typical optimal solution for relatively high impact velocities (penetration into nonfrozen soil, rock, and concrete shields, $m_{\text{imp}} = 400\,\text{kg}$, $m_{\text{res}} = 200\,\text{kg}$, $v_{\text{imp}} = 700\,\text{m/s}$); (a–b) optimal burning programs; (c) normalized optimal DOP versus $\bar{\beta}_{\min}$. (H is DOP for the optimal burning program, H_0 is DOP for a passive trajectory.)

7. Concluding remarks

We suggested a mechanical model of a penetrator equipped with a jet thruster and demonstrated that appropriate choice of the parameters of a jet thruster allows increasing the depth of penetration considerably into different media. We showed that for relatively small impact velocities (about 100 m/s), penetration at the maximum depth is attained with velocities lower than the impact velocity. Nelson [2002] emphasized that there is a limitation on increasing impact velocity in order to attain a higher penetration depth because of the constraints on the impact velocity required for the survival of a penetrator on impact. Using a jet thruster is one of the possible solutions to overcome this constraint.

References

[Bellman et al. 1958] R. E. Bellman, I. Glicksberg, and O. A. Gross, *Some aspects of the mathematical theory of control processes*, Rand Corp., Santa Monica, Calif., 1958.

[Ben-Dor et al. 2005] G. Ben-Dor, A. Dubinsky, and T. Elperin, "Ballistic impact: recent advances in analytical modeling of plate penetration dynamics. A review", *Appl. Mech. Rev.* (*Trans. ASME*) **58**:6 (2005), 355–371.

[Ben-Dor et al. 2006] G. Ben-Dor, A. Dubinsky, and T. Elperin, *Applied high-speed plate penetration dynamics*, Springer, Dordrecht, 2006.

[Ben-Dor et al. 2007] G. Ben-Dor, A. Dubinsky, and T. Elperin, "Optimization of high-speed penetration by impactor with jet thruster", *Mech. Based Des. Struct. Mach.* **35**:3 (2007), 205–228.

[Cicala and Miele 1956] P. Cicala and A. Miele, "Generalized theory of the optimum thrust programming for the level flight of a rocket-powered aircraft", *ARSJ Am. Rocket Soc. J.* **26**:6 (1956), 443–455.

[Eisler et al. 1998] R. D. Eisler, A. K. Chatterjee, G. H. Burghart, and P. Loan, "Simulates the tissue damage from small arms projectiles and fragments penetrating the musculoskeletal system", Final report, Mission Research Corp, Fountain Valley, CA, 1998.

[Gould 1997] R. L. Gould, "Penetrating vehicle with rocket motor", U.S.A. Patent 5596166, 1997.

[Hibbs 1952] A. R. Hibbs, "Optimum burning program for horizontal flight", *ARSJ Am. Rocket Soc. J.* **22**:4 (1952), 204–212.

[Kosmodemiansky 1966] A. A. Kosmodemiansky, *Course on theoretical mechanics. Part 2*, Prosveschenije, Moscow, 1966. in Russian.

[Krotov 1995] V. F. Krotov, *Global methods in optimal control theory*, Marcel Dekker, New York, 1995.

[Leitmann 1962] G. Leitmann, *Optimization techniques with applications to aerospace systems*, Academic Press, New York, London, 1962.

[Miele 1957] A. Miele, "An extension of the theory of the optimum burning program for the level flight of a rocket-powered aircraft", *J. Aerospace Eng.* **24**:12 (1957), 874–884.

[Miele 1962] A. Miele, "The calculus of variations in applied aerodynamics and flight mechanics", pp. 258–301 in *Optimization techniques with applications to aerospace systems*, edited by G. Leitmann, Academic Press, New York, London, 1962.

[Nelson 2002] R. W. Nelson, "Low-yield earth-penetrating nuclear weapons", *Sci. Global Secur.* **10**:1 (2002), 1–20.

[Pedregal 2003] P. Pedregal, *Introduction to optimization*, Springer, New York, 2003.

[Sagomonyan 1988] A. Y. Sagomonyan, *Dynamics of barriers perforation*, Moscow Univ. Publ., Moscow, 1988. in Russian.

[Tertychny-Dauri 2004] V. Y. Tertychny-Dauri, *Hyperreactive mechanics*, Fizmatlit, Moscow, 2004. in Russian.

[Young 1997] C. W. Young, "Penetration equations", Report No. SAND972426, Sandia Nat. Lab., Albuquerque, NM, 1997.

Received 13 Aug 2007. Accepted 21 Jan 2008.

GABI BEN-DOR: bendorg@bgu.ac.il
Pearlstone Center for Aeronautical Engineering Studies, Department of Mechanical Engineering, Ben-Gurion University of the Negev, P.O. Box 653, Beer-Sheva, 84105, Israel
http://eng2.bgu.ac.il/engineering/profile.aspx?id=juesiMMt

ANATOLY DUBINSKY: dubin@bgu.ac.il
Pearlstone Center for Aeronautical Engineering, Department of Mechanical Engineering, Ben-Gurion University of the Negev, P.O. Box 653, Beer-Sheva, 84105, Israel
http://www.bgu.ac.il/∼dubin

TOV ELPERIN: elperin@bgu.ac.il
Pearlstone Center for Aeronautical Engineering, Department of Mechanical Engineering, Ben-Gurion University of the Negev, P.O. Box 653, Beer-Sheva, 84105, Israel
http://www.bgu.ac.il/me/staff/tov/index.html